ROS

RESEARCH ARTICLE

Manganese-Containing Thiocarbamates Cause Free Radical Production and Caspase-Independent Cell Death following Mitochondrial Dysfunction in Neural Cells

R. Nisar[1], P.S. Hanson[1], P.C. Keane[1], L. He[2], R.W. Taylor[2], P.G. Blain[1], and C.M. Morris[1]

[1]Medical Toxicology Centre and National Institute for Health Research Health Protection Research Unit in Chemical and Radiation Threats and Hazards, Newcastle University, Claremont Place, Newcastle upon Tyne, NE2 4AA, UK; [2]Wellcome Trust Centre for Mitochondrial Research, Institute of Neuroscience, The Medical School, Newcastle University, Framlington Place, Newcastle upon Tyne, NE2 4HH, UK

Correspondence: c.m.morris@ncl.ac.uk (C.M.M.)

Nisar R et al. Reactive Oxygen Species 6(18):428–444, 2018; ©2018 Cell Med Press
http://dx.doi.org/10.20455/ros.2018.871
(Received: July 31, 2018; Revised: August 12, 2018; Accepted: August 14, 2018)

ABSTRACT | Maneb and mancozeb are some of the most commonly used fungicides. However, there is concern that chronic maneb or mancozeb exposure has been linked with parkinsonism through generation of reactive oxygen species (ROS). In order to study this further we investigated the capacity of maneb and mancozeb to induce cell death and parkinsonian changes using in vitro cell models. Results indicate that maneb and mancozeb are acutely toxic at concentrations as low as 10 µM to SH-SY5Y cells. The mode of cell death appears to be via a caspase-independent mechanism, possibly programmed necrosis, and production of ROS through inhibition of complex III of the mitochondrial respiratory chain. This toxicity is accompanied by lysosomal enlargement although inhibition of autophagy had no effect on cytotoxicity and no accumulation of α-synuclein was seen. Such changes indicate that while toxic, maneb and mancozeb may have limited potential to induce classical Lewy body Parkinson's disease due to lack of synuclein accumulation but may achieve toxicity via ROS production and mitochondria-mediated cell death.

KEYWORDS | Apoptosis; Mancozeb; Mitochondria; Necrosis; Parkinson's disease; Reactive oxygen species; Synuclein; Thiocarbamate

ABBREVIATIONS | ATP, adenosine triphosphate; CMA, chaperone-mediated autophagy; cyt c, cytochrome c; DTC, dithiocarbamate; H_2DCFDA, 2′,7′-dichlorodihydrofluorescein diacetate; LAMP, Lysosome-associated membrane protein; 3-MA, 3-methyl adenine; MPP^+, 1-methyl-pyridinium ion; NAC, *N*-acetyl-cysteine; Nec-1, necrostatin-1; PD, Parkinson's disease; PARP-1, poly(ADP-ribose) polymerase 1; ROS, reactive oxygen species; TH, tyrosine hydroxylase; TMRE, tetramethylrhodamine ethyl ester

CONTENTS

1. INTRODUCTION

The thiocarbamate fungicides, particularly dithiocarbamates such as maneb [manganese ethylenebis(dithiocarbamate)], mancozeb [manganese-zinc ethylenebis(dithiocarbamate)], and zineb [zinc ethylenebis(dithiocarbamate)], are extensively used for plant protection, with an estimated 5.5 million kilograms of maneb and mancozeb applied annually [1]. Chronic maneb exposure has been associated with parkinsonism [2, 3], and dithiocarbamates (DTCs) generally have been linked clinically to several extrapyramidal syndromes [2] and a variety of neurobehavioral abnormalities (hind limb paralysis, convulsions, ataxia, hemiparesis) experimentally [4]. One finding from epidemiological studies is the suggestion that Parkinson's disease (PD) may have an environmental component and that pesticide exposure may be a cause [3]. DTCs are suggested to exert their parkinsonian toxicity through dopamine catalysis and oxidative stress following metal chelation although other mechanisms have been suggested [5]. Details about neurotoxicity are, however, unclear as maneb can inhibit glutamate transport, interfere with dopamine uptake and release [6], and is also suggested to inhibit the mitochondrial electron transport chain. Like 1-methyl-pyridinium ion (MPP^+), a known PD-causing toxin [7, 8], maneb causes striatal dopamine influx [9], and short term maneb exposure can cause a reduction in adenosine triphosphate (ATP) levels suggesting inhibition of energy metabolism and mitochondrial respiration and production of reactive oxygen species (ROS) [10]. Both maneb and mancozeb are toxic in vitro to dopaminergic and GABAergic cell populations, acting as inhibitory uncouplers, uncoupling and inhibiting respiration at low doses and completely inhibiting respiration at high doses (30 mM) leading to a dose-dependent reduction in tyrosine hydroxylase (TH)-positive cell number along with decrease in neurite length [10]. The precise aspects of DTCs on mitochondrial function have, however, not been well described.

Limited data is available showing how DTCs may link to cell death/survival programs such as apoptosis, necrosis, or autophagy. The autophagy gene *ATG5* encodes a critical protein needed at the stage of autophagosome-precursor synthesis and *ATG5* deletion in yeast or mammalian cells effectively blocks autophagy [11, 12]. Similarly, *ATG5* down-regulation in HeLa cells can reduce cell death and vacuole formation induced by interferon-gamma (IFN-γ) [13]. Mitophagy, the selective removal of damaged mitochondria, may be one route which links PD, mitochondrial dysfunction, and programmed cell death. Lysosome-associated membrane proteins-1 and -2 (LAMP1, LAMP2) are lysosome-specific transmembrane proteins required for autophagolysosome formation during mitophagy [14]. It has been suggested

that down-regulation of LAMP1/2 can increase sensitivity to lysosome-mediated cell death [15]. Therefore, the aim of this study was to investigate the effect of selected DTCs on SH-SY5Y cells to determine the major mode of cell death and to determine if inhibition of mitochondrial function, production of ROS, and autophagy/mitophagy plays a part in any cell death process.

2. MATERIALS AND METHODS

2.1. Cell Culture

Maneb, mancozeb, zineb, and nabam were of technical grade and obtained from Sigma-Aldrich (Poole, UK). The SH-SY5Y cell line was purchased from the European Collection of Cell Cultures (Salisbury, UK), and maintained in a growth medium containing 90% Dulbecco's modified Eagle's medium (DMEM), 10% fetal bovine serum, 2 mM L-glutamine, 100 units/ml of penicillin, 10 µg/ml of streptomycin, and 1% non-essential amino acids (NEAA). Cells were subcultured when growth reached 80–90% confluence. Cells were incubated at 37ºC in a humidified atmosphere of 95% air and 5% CO_2. SH-SY5Y cells were seeded at 100,000 cells per well in 24- or 48-well plates and used after 24 h. An initial dose range of 10 nM–1 mM was used for each chemical. Following overnight exposure to chemicals, Alamar Blue (0.01% rezasurin; Sigma-Aldrich) was added at 10% of total growth medium volume and plates were incubated at 37°C and 5% CO_2 for 4 h. Alamar blue reduction was then measured at an excitation wavelength of 530 nm and emission wavelength of 590 nm. Cell numbers were also estimated as necessary using direct cell counting of cells stained with 0.5% trypan blue.

2.2. Determination of Cell Viability in Response to Cell Signaling/Death Inhibitors

Mancozeb, maneb, zineb, and nabam concentrations causing a reduction of approximately 50% in viability were used and assessed using Alamar Blue reduction. SH-SY5Y cells were incubated with necrostatin-1 (Biomol, Kelayres, PA, USA), z-VAD.fmk (Biomol), DEVD-CHO (Biomol), Ac-LEVD-CHO (Biomol), *N*-acetyl-cysteine (NAC) (Sigma-Aldrich), cyclosporine A (Sigma-Aldrich), tunicamycin (Sigma-Aldrich), 3-methyladenine (Sigma-Aldrich), ammonium chloride (Sigma-Aldrich), or tiron (Sigma-Aldrich) for 3 h prior to toxin administration. Cell viability was then assessed using Alamar Blue reduction assay 18 h after toxin response in the continuous presence of the inhibitor.

2.3. Acute and Chronic Toxin Exposure

SH-SY5Y cells were plated as described previously and exposed to sub-cytotoxic doses of maneb or mancozeb for 24 h (acute exposure) or continuously for 4 weeks (chronic exposure). Cell lysates were prepared using native lysis buffer (50 mM Tris-HCl, pH 7.4, containing 0.27 M sucrose, 1% Triton X-100, and 1× protease/phosphatase inhibitor cocktail). The protein concentration was determined by Bradford assay (Pierce, Cramlington, UK).

2.4. Western Blotting

Equal amounts of protein (20 µg), were subjected to electrophoresis through 12% Bis-Tris gels (Invitrogen, Carlsbad, CA) at 120 V for 1 h. After electrophoresis, proteins were transferred onto nitrocellulose membranes (Amersham Biosciences, Little Chalfont, UK). Membranes were blocked for 1 h with 5% non-fat dry milk in 1× TBS-Tween 20 (0.2% v/v) (TBS-T) and probed overnight at 4°C with primary antibodies. Membranes were washed 3 times with TBS-T at room temperature for 10 min, followed by incubation with HRP-conjugated secondary antibodies (rabbit IgG or mouse IgG, AbCam, Cambridge, UK) for 1 h at room temperature. Membranes were thoroughly washed with TBS-T. An ECL detection kit (GE Healthcare, Chicago, IL, USA) was used for protein band detection through a G:BOX Chemi XL camera (SYNGENE, Cambridge, UK). The ImageJ version 1.38x (NIH, Bethesda, USA) was used to quantify each protein band.

2.5. Determination of ROS Generation

To detect cellular ROS, SH-SY5Y cells were loaded with 2′,7′-dichlorodihydrofluorescein diacetate (H_2DCFDA) (10 µM, Molecular Probes, Invitrogen) and treated with hydrogen peroxide (0.5 mM) positive control, maneb or mancozeb, (dose range: 1 µM to 1 mM) overnight. H_2DCFDA is known to react with hydrogen peroxide in the presence of cellular

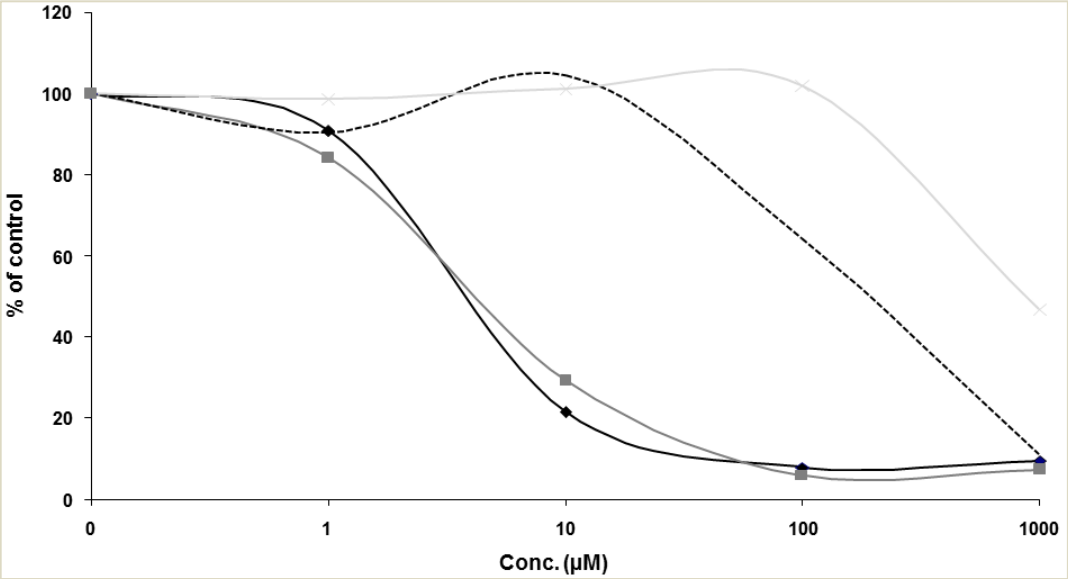

FIGURE 1. Viability of SY5Y cells exposure to dithiocarbamate fungicides. Shown is the dose-response effect of acute mancozeb (—♦—), maneb (—■—), nabam (—x—), and zineb (----) on SH-SY5Y cell viability. All chemicals caused decrease in viability in a dose-dependent manner with maneb and mancozeb showing toxicity at concentrations as low as 1 μM.

peroxidases, peroxynitrite ($ONOO^-$), and with other cellular peroxy-compounds to produce the fluorescent 2′,7′-dichlorofluorscein product [16, 17]. Plates were incubated at 37°C and 5% CO_2 for 24 h after which triplicates were taken from each well and fluorescence measured at an excitation wavelength of 485 nm and an emission wavelength of 520 nm. After toxin treatment SH-SY5Y cells were also extracted in 0.1 M Tris-HCl buffer, pH 7.4, containing 1% Triton X-100, and cell lysate fluorescence was measured as above.

2.6. Analysis of Mitochondrial Membrane Potential

Changes in mitochondrial membrane potential ($\Delta\Psi_m$) were estimated using tetramethylrhodamine ethyl ester (TMRE; Invitrogen) [18]. Cells were incubated with 250 nM TMRE for 30–45 min at 37°C and fluorescence was measured (excitation at 549 nm and emission at 574 nm). Protonophore carbonyl cyanide *p*-trifluoromethoxy-phenylhydrazone (FCCP; 0.1 μM, Sigma-Aldrich) was used as a positive control and added 15 min prior to the end of cell treatment to cause mitochondrial depolarization [19]. The fluorescence for each treatment was expressed as percent fluorescence change compared with control.

2.7. Preparation of Mitochondrial Fraction from SH-SY5Y Cells

SH-SY5Y cells were grown to 80–90% confluence and the cells removed with a cell scraper and the pellet suspended in 1–2 ml of ice-cold medium containing 250 mM sucrose, 2 mM HEPES, 0.1 mM EGTA, pH 7.4, and transferred to a 1–2 ml capacity smooth-surfaced glass homogenizer. Cells were disrupted by 20 passes in the homogenizer with a tight-fitting power-driven Teflon plunger and the homogenates were then centrifuged for 10 min at 600 *g* at 4ºC. Mitochondria-rich supernatant was collected and the pellet containing the cell debris resuspended in 800 μl homogenization medium and homogenized and centrifuged as previously. The two supernatants were pooled and centrifuged for 10 min at 11,000 *g* at 4ºC. The pellet (mitochondrial fraction) was resuspended in 400 μl homogenization medium and stored as aliquots at –80ºC.

Respiratory chain complex assays were performed in a final volume of 0.1 ml using a Cary WinUV spectrophotometer using methods for the clinical investigation of mitochondrial activity [20, 21]. Pig heart mitochondrial fractions were used as internal control before each experiment to assess normal function of assays. For measurement of complex I (NADH:ubiquinone oxidoreductase) activity, the decrease in absorbance due to the oxidation of NADH at 340 nm was followed. Complex I activity was calculated as the rotenone-sensitive NADH:ubiquinone oxidoreductase activity [20, 21]. Measurement of mitochondrial complex II (succinate:ubiquinone oxidoreductase) activity was measured by following the reduction of 2,6-dichlorophenol-indo-phenol (DCPIP) at 600 nm. Complex III activity was measured by determining the oxidation of ubiquinol-2 with cytochrome c III (cyt c III) as the electron acceptor and monitoring the increase in absorbance due to the reduction of cyt c III at 550 nm. Complex IV activity was determined as oxidation of reduced cytochrome c (II) at 550 nm. Citrate synthase activity was determined by following the rate of production of coenzyme A from oxaloacetate via measuring free sulfhydryl groups using the thiol-reactive reagent 5,5′-dithiobis(2-nitrobenzoic acid) (DTNB) at 412 nm [20, 21].

2.8. Cellular Distribution of Mitochondria

SH-SY5Y cells were seeded onto 2-well chamber slides (BD Biosciences, Franklin Lakes, NJ, USA) and allowed to recover overnight before loading with MitoTracker® Red CMXRos (Molecular Probes, Invitrogen) for 30 min. Growth media were replaced and maneb and mancozeb added at the required concentrations and incubated for 24 h after which cells were fixed with 1% paraformaldehyde in phosphate-buffered saline (PBS) and viewed using a fluorescent microscope.

2.9. Immunofluorescent Analysis of Lysosomal Aggregation

SH-SY5Y cells were seeded onto 2- or 8-well chamber slides (BD Biosciences) and incubated with LysoTracker® Red DND-99 (Molecular Probes, Invitrogen) (1 µM) for 30 min. Chemicals were added and incubated for 24 h after which cells were fixed and viewed using a fluorescent microscope.

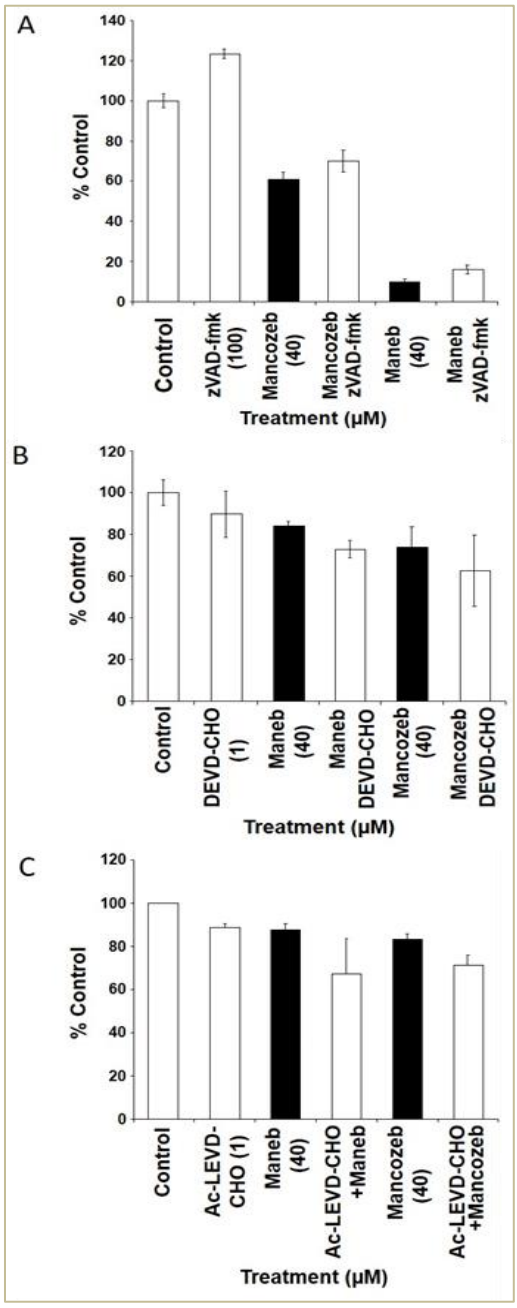

FIGURE 2. Effect of caspase inhibition on cell viability in DTC-induced cytotoxicity. Cells were pre-incubated with (A) zVAD.fmk (1 µM), (B) DEVD-CHO (1 µM), or (C) Ac-LEVD-CHO (1 µM) for 3 h before maneb or mancozeb addition. After 24 h incubation, cell viability was evaluated by Alamar Blue reduction assay. The data are expressed as mean ± SD (n = 3).

TABLE 1. Percentage change of cell viability in toxin-treated cells after cell signaling inhibition

Inhibitor	Maneb	Mancozeb
Nec-1	+19.5 ± 18.7*	+35.6 ± 4.5*
zVAD.fmk	+0.6 ± 4.9	+4.1 ± 8.7
NAC	+30 ± 8.6*	+53 ± 16.9*
Cyclosporine A	–14 ± 7.7	–1 ± 1
3-Methyladenine	–4.5 ± 2.2	–5 ± 2.3
Ammonium Chloride	+3.35 ± 0.07	0.6 ± 2.0
Tiron	+4.3 ± 0.6	+7.0 ± 10.6

Note: Cells were pre-incubated with inhibitors for 3 h before compound addition. After 24 h incubation, cell viability was evaluated by Alamar Blue reduction assay. The data are expressed as mean ± SD of at least 3 independent experiments. *, $p < 0.05$ compared with the toxin-treated group in the absence of the inhibitor. The plus sign indicates increase in cell viability, and the minus sign denotes reduction of cell viability.

2.10. Immunofluorescence

SH-SY5Y cells were seeded onto 2-well chamber slides (BD Falcon, BD Biosciences) and incubated with compounds after which cells were fixed with 4% paraformaldehyde (Sigma-Aldrich) for 10 min and washed with PBS and permeabilized with 0.1% Triton-X-100 (Sigma-Aldrich) for 10 min. Cells were blocked in 1% bovine serum albumin (BSA) or 10% goat serum for 30 min, and incubated overnight with primary antibodies at 4ºC, washed with PBS and treated with Image-iT™ FX signal enhancer (Invitrogen) for 30 min at room temperature. Cells were washed with PBS and then incubated with secondary antibodies (conjugated with Alexa Fluor® 488 or 594) for 60 min. Slides were washed with PBS and viewed using a fluorescent microscope.

2.11. Statistical Analysis

Results are expressed as the mean ± standard deviation (SD) of at least three independent experimental replicates. The statistical significance was determined by ANOVA followed by post-hoc t-test when appropriate. A p value less than 0.05 was considered statistically significant.

3. RESULTS

3.1. Cytotoxicity of Maneb and Mancozeb

SH-SY5Y cells were treated with varying compound concentrations (1 µM to 1 mM) for 24 h. Significant toxicity was observed at 10 µM with maneb and mancozeb (**Figure 1**), though zineb and nabam showed lower toxicity, while the metabolite 2-imidazolidinethione showed minimal toxicity to SH-SY5Y cells (> 1 mM; data not shown). Cell viability measured using Alamar Blue at different time points of exposure also showed a time-dependent decrease in cell viability. No toxic effects as determined by a reduction in cell viability or morphological changes were observed in the first 2 h of exposure. A reduction of nearly 20% (of untreated control) was measured after 4 h exposure with maneb and mancozeb, followed by a drop in viability to 50% and to 5–10% after 6 and 24 h, respectively. Cell counts determined by trypan blue exclusion showed similar proportional reductions in cell number for 100 µM and 1 mM for both maneb and mancozeb (data not shown).

3.2. Effect of Cell Death Inhibitors on Cytotoxicity

SH-SY5Y cells were treated with toxins or vehicle dimethyl sulfoxide (DMSO) in the presence or absence of specific caspase-3/9 inhibitors and z-VAD-fmk, a cell-permeable broad-spectrum caspase inhibitor, to determine if apoptosis is induced by DTCs [22]. Z-VAD-fmk treatment showed a slight reduction in toxicity of maneb and mancozeb which was not statistically significant (**Figure 2**). Similarly, treatment with the specific caspase-3 inhibitor DEVD-CHO or the caspase-9 inhibitor Ac-LEVD-CHO also failed to affect toxicity (**Figure 2**), suggesting apoptosis is not a major feature of DTC-induced cell death in this cell line. Caspase-3 plays a

role in proteolytic cleavage of several downstream mediators of cell death and caspase-3 cleavage is required for its activation; however, Western blotting failed to detect the large fragment (17/19 kDa) of activated caspase-3 following maneb or mancozeb treatment (not shown).

As previous studies have shown that caspase inhibition does not always protect against apoptosis, we investigated alternative cell death processes [23, 24]. Since autophagy may be responsible for cell death caused by a chemical insult and can be prevented by using autophagy inhibitors [25], we investigated this mechanism. Pretreatment of SH-SY5Y cells with 3-methyl adenine (3-MA; 1.5, 2.5, and 5 mM) as an inhibitor of macroautophagy failed to prevent cell death (**Table 1**). Previous studies indicate that autophagy can be abolished by complete knockout of *ATG5*, and the formation of autophagic vacuoles can be reduced through lower ATG5 protein expression [26]. *ATG5* siRNA-mediated knockdown significantly reduced ATG5 protein expression to 40% of untransfected control and completely blocked LC3-II expression (**Supplementary Figure 1**). A significant decrease ($p < 0.05$) in Alamar Blue reduction was noticed in siRNA transfected cells (75% ± 2.2 of controls) after 72 h. Cell viability was measured after a further 24 h treatment with DTCs, and the overall results indicated no significant increase or reduction ($p > 0.05$) in cell viability in ATG5-knock down cells treated with maneb or mancozeb (**Supplementary Figure 1**). Acute exposure of cells to maneb or mancozeb also failed to change the endogenous levels of ATG5 protein (**Supplementary Figure 1**).

Lysosome-associated membrane proteins-1 and -2 (LAMP1, LAMP2) are lysosome-specific transmembrane proteins required for autophagolysosome formation and mitophagy [14]. It has been suggested that down-regulation of LAMP1/2 can increase sensitivity to lysosome-mediated cell death [15]. LAMP1 levels were measured after 24 h toxin exposure, and results showed a significant increase ($p < 0.05$) after maneb (1, 10, and 100 µM) and mancozeb (10, 50, and 75 µM; **Figure 3**). Similarly, LAMP2 levels measured after 24 h toxin exposure showed a significant increase ($p < 0.05$) after high dose maneb (100 µM) and mancozeb (100 µM) treatment (**Supplementary Figure 2**). To investigate the distribution of lysosomes after compound treatment, SH-SY5Y cells were incubated with LysoTracker® red DND-99 to label acidic organelles. Media-treated

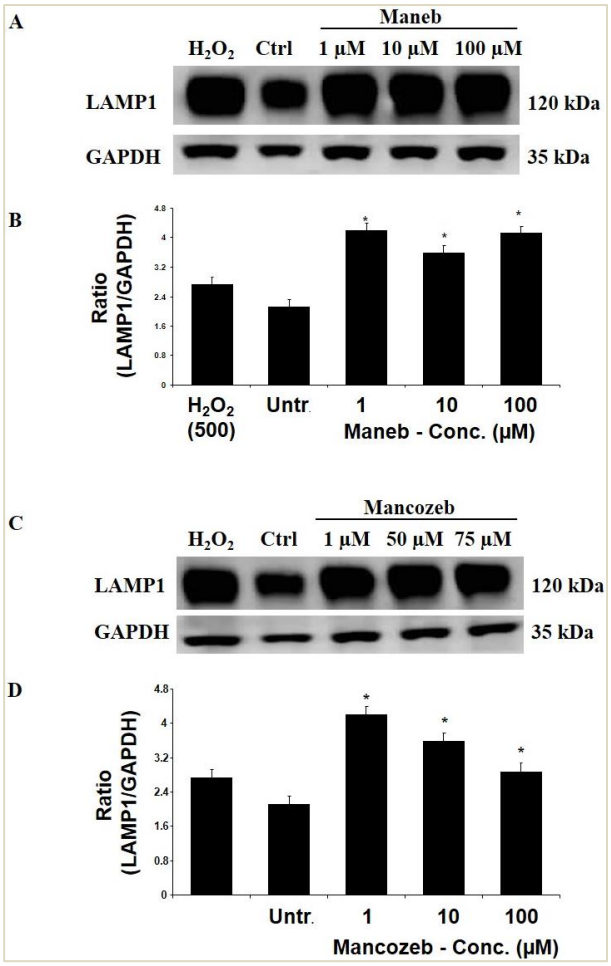

FIGURE 3. Toxin-induced changes in LAMP-1 levels. SH-SY5Y cells were treated with different doses of maneb (A and B) or mancozeb (C and D) for 24 h after which cell extracts were probed for LAMP-1 protein. Data in panels B and D are expressed as mean ± SD of three independent replicates. *, $p < 0.05$ compared with untreated control.

control cells showed a uniform distribution of fluorescent bodies in the cytoplasm whereas 24 h treatment including exposure to H_2O_2 (100 µM), maneb (50 µM) or mancozeb (50 µM) showed the presence of large cytoplasmic aggregates (**Figure 4**). Aggregate formation was dose- and time-dependent with cells exposed to maneb for 24 h showed a relatively smaller number of stained bodies when treated with 10 µM, but the size of these increased when treated

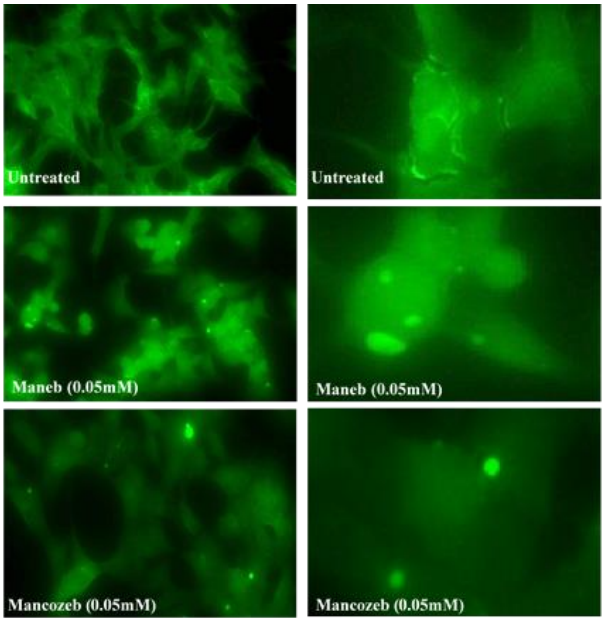

FIGURE 4. Localization of lysosomal aggregates after toxin treatment. Treatment with maneb or mancozeb for 24 h resulted in the formation of lysosomal aggregates which were stained with LysoTracker® DND-99 and viewed under a fluorescent microscope (magnification: ×40; for right hand side panel, selected cells were magnified to show enlargement).

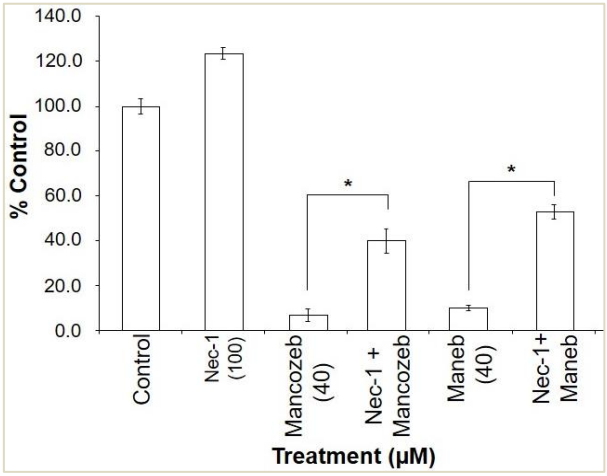

FIGURE 5. Effect of necrostatin-1 on cell viability in toxin-induced cytotoxicity. Cells were pre-incubated with necrostatin-1 (100 µM) for 3 h before compound addition. After 24 h incubation, cell viability was evaluated by Alamar Blue reduction assay. The data are expressed as mean ± SD of at least three independent experiments. *, $p < 0.05$ compared with the indicated group.

at 100 µM (**Figure 4**). Treatment of cells with ammonium chloride in order to prevent lysosomal acidification was, however, without effect in SH-SY5Y cells treated with maneb or mancozeb (**Table 1**).

Since caspase or autophagy inhibition failed to prevent cell death with maneb or mancozeb, we sought to identify alternative cell death pathways. Necrostatin-1 (Nec-1) as an inhibitor of programmed necrosis was used, and Nec-1 (100 µM) showed a significant reduction of cell death with maneb and mancozeb (**Figure 5** and **Table 1**). Nec-1 caused a 20% reduction in maneb and 35% reduction in mancozeb toxicity in treated cells (**Table 1**). Since Nec-1 is thought to have its main mode of action via inhibition of the kinase RIP1 [27], identification of changes in the RIP1 expression was undertaken. Immunostaining of RIP1 showed extra-nuclear distribution of RIP1 in SH-SY5Y cells though no change in its localization was observed between untreated cells and those exposed to mancozeb (50 µM), maneb (50 µM), or MPP^+ (100 µM; not shown). The endogenous levels of total and cleaved RIP1 protein were measured after treatment which showed a significant increase in the levels of full length RIP1 ($p < 0.05$; **Figure 6**) in mancozeb-treated cells (10 and 100 µM) compared with untreated cells, and, although reduced, there was no significant difference in cleaved RIP1 (~45kDa) in untreated and treated cells (data not shown). Maneb showed similar changes to mancozeb with significant increase for full length RIP1 but no change in cleaved RIP1 levels.

3.3. Effect of Acute Toxin Exposure on Mitochondrial Respiratory Chain Activity

Acute mancozeb or maneb exposure can inhibit ATP production before major toxicity effects take effect [10]. Exposure of SH-SY5Y cell-derived mitochondria to lower (1 µM) or higher (1 mM) doses of maneb or mancozeb had no significant effect on complex I or II activity (**Table 2**). Complex III activity was, however, inhibited by maneb exposure, alt-

hough high dose exposure did not affect complex IV activity (**Table 3**). Further investigation of rate of reaction inhibition suggests that maneb reduces the rate of transfer of electrons from complex III to cytochrome c.

To investigate the effect of toxin exposure on mitochondrial distribution, SH-SY5Y cells were incubated with MitoTracker® Red CMXRos before 24 h toxin treatment with mancozeb (50 µM) or maneb (50 µM) (**Figure 7**). Results showed large cytoplasmic aggregates in treated cells compared with uniform distribution of small punctate areas in untreated cells. Despite the changes in mitochondrial distribution, no change in mitochondrial transmembrane potential was seen when assessed using TMRE fluorescence (data not shown). Use of the mitochondrial transition permeability pore inhibitor cyclosporine A also failed to prevent DTC-mediated cell death (**Table 1**).

3.4. Increased ROS in Toxin-Treated Cells

Since mitochondrial inhibition and also programmed necrosis often lead to production of ROS, H_2DCFDA was used to detect a number of ROS, including peroxynitrite and hydroxyl radical through the production of 2',7'dichlorofluoroscein [16, 17, 28]. Maneb and mancozeb showed increased DCF production with a dose range of 1–100 µM (**Figure 8**). The glutathione precursor NAC significantly increased cell survival in the presence of maneb and mancozeb; however, the use of the ROS scavenger tiron did not significantly improve cell survival for maneb or following mancozeb exposure (**Table 1**).

To determine if oxidative stress caused by maneb and mancozeb could lead to DNA damage, a range of different cell death markers were determined using Western blotting following toxin treatment, their absence or presence indicating the mode of cell-death. Poly(ADP-ribose) polymerase 1 (PARP-1, 116 kDa) is a nuclear enzyme involved in DNA repair in response to cellular stress [29] which can be cleaved by caspase-3 [30, 31]. Using an antibody to the 89 kDa cleaved fragment, treatment with maneb and mancozeb showed PARP-1 cleavage at 1, 10, and 100 µM only after 24 h exposure (**Supplementary Figure 3**), suggesting that DNA damage is a downstream event compared to the process of cell death initiation which occurs after 2–4 h exposure. Free radical generation and oxidative stress have an

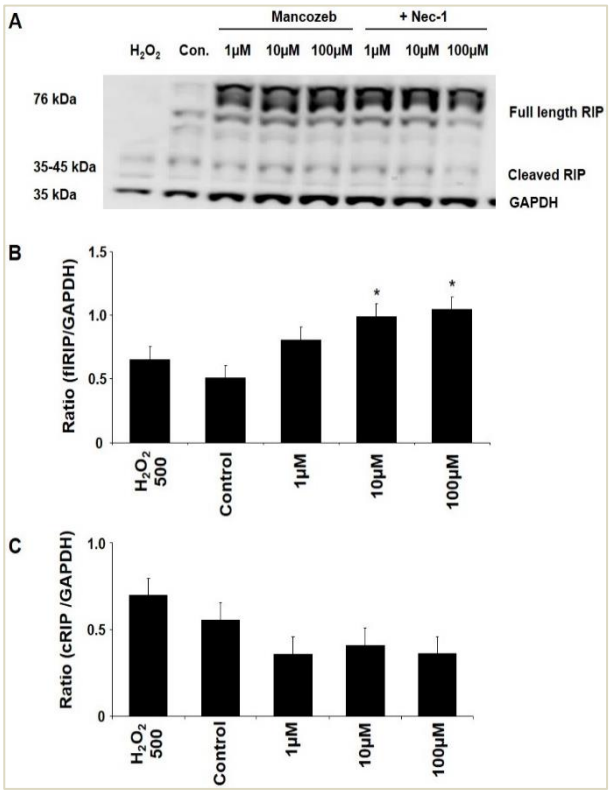

FIGURE 6. Toxin-induced changes in RIP1 levels. SH-SY5Y cells (± Nec-1) were treated with (A-C) mancozeb, for 24 h after which cell extracts were probed for RIP1. The data in panels B and C are expressed as mean ± SD (n = 3). *, $p < 0.05$ compared with untreated control.

effect in causing a DNA-damage response in cells. Protein levels of p53 can be elevated through accumulation of DNA strand breaks which can also activate p53-mediated signaling pathways [32]. Protein expression in SH-SY5Y cells after 24 h toxin treatment showed significant elevation of total p53 protein ($p < 0.05$) after treatment with mancozeb (75 µM) and maneb (10 and 100 µM) (**Supplementary Figure 4**).

3.5. Effect on α-Synuclein

Since α-synuclein deposition in the form of Lewy bodies is a key feature of PD, we determined if α-synuclein may be involved in the response to maneb or mancozeb treatment, and total α-synuclein and α-

TABLE 2. Mean complexes I and II activity in toxin-treated SH-SY5Y cell-derived mitochondria

Sample	Conc. (µM)	Mean complex I (CI) activity (µmol/min)	Mean complex II (CII) activity (µmol/min)	CI/CII
Control (+ rotenone)	5 µM	0.011 ± 0.013	0.062 ± 0.001	0.19
Maneb	1 µM	0.021 ± 0.001	0.047 ± 0.001	0.44
Maneb	1 mM	0.031 ± 0.001	0.032 ± 0.002	0.95
Mancozeb	1 µM	0.018 ± 0.000	0.026 ± 0.001	0.96
Mancozeb	1 mM	0.016 ± 0.003	0.042 ± 0.001	0.38

Note: Complex I (µmol of NADH oxidized/min) and complex II activity (µmol of DCPIP reduced/min) after maneb (1 µM and 1 mM) or mancozeb (1 µM and 1 mM) treatment. Data are expressed as mean ± SD (n = 3).

TABLE 3. Mean complex III and complex IV activity in maneb-treated SH-SY5Y cell-derived mitochondria

Sample	Conc. (µM)	Mean complex III activity (10^{-3} K.sec^{-1})	Mean complex IV activity (10^{-3} K.sec^{-1})
Untreated	0	0.027 ± 0.002	8.63 ± 0.61
Maneb	5 µM	0.014 ± 0.002*	ND
Maneb	50 µM	0.08 ± 0.001*	ND
Maneb	500 µM	0.001 ± 0.001**	6.90 ± 0.66

Note: First order rate constants for complex III (µmol of cytochrome c III) and complex IV activity (µmol of cytochrome c II) after maneb (5, 50, and 500 µM) treatment. Data are expressed as mean ± SD (n = 3). *, $p < 0.05$; **, $p < 0.01$, compared with untreated control. ND denotes not detectable.

synuclein phosphorylated at Ser129 were assessed after 24 h treatment. Immunoblots showed a single 19kDa total α-synuclein band and also heavy bands between 40 kDa and 55kDa with anti-α-synuclein and anti-phosphorylated α-synuclein antibodies, respectively. Treatment with maneb and mancozeb showed no change in protein levels (**Supplementary Figure 5**). Immunocytochemical analysis from previous studies has shown that rotenone treatment increases the amount of cellular α-synuclein in apoptotic cells [33] and chronic treatment with 50 nM rotenone can form neuritic swellings morphologically resembling the α-synuclein immunoreactive Lewy neurites seen in PD brain tissue [34]. As above, acute toxin exposure failed to change α-synuclein levels. Therefore, cells were grown in medium containing lower doses of maneb (1 µM) or mancozeb (1 µM) continuously for 4 weeks, but analysis of protein expression showed no significant change in α-synuclein levels (**Supplementary Figure 5**).

4. DISCUSSION

Our findings are consistent with previous reports showing significant cellular toxicity with maneb and mancozeb in dopaminergic and GABAergic neurons accompanied with a decrease in TH-positive neuritic processes, but not with nabam [10]. DTC fungicides share a common backbone, and only the addition of a specific metal ion gives it a characteristic identity [10]. Mancozeb contains manganese and zinc ions and is slightly more toxic than maneb suggesting that the organic moiety and the metal components produce the toxic effects. Zineb's organic structure is identical to maneb but is significantly less toxic than maneb. Similarly, nabam, containing the organic backbone with sodium, shows reduced toxicity. This suggests that manganese component of mancozeb/maneb as the "cytotoxicity inducing portion" of the chemical [6] since studies have shown that mancozeb inhibits glutamate uptake more potently

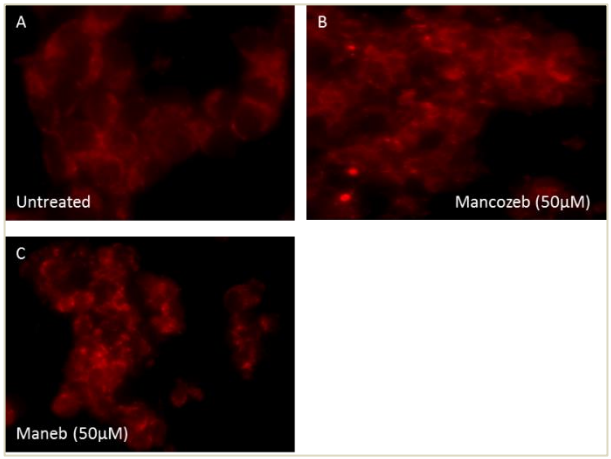

FIGURE 7. Mitochondrial localisation after toxin treatment. SH-SY5Y cells were treated with selected toxins after staining with MitoTracker® Red CMXRos and viewed under a fluorescent microscope (magnification: ×40). In untreated cells, an even distribution of small punctate cytoplasmic mitochondria was observed (A) and in mancozeb- or maneb-treated cells, mitochondria clustered in large cytoplasmic aggregates (B and C).

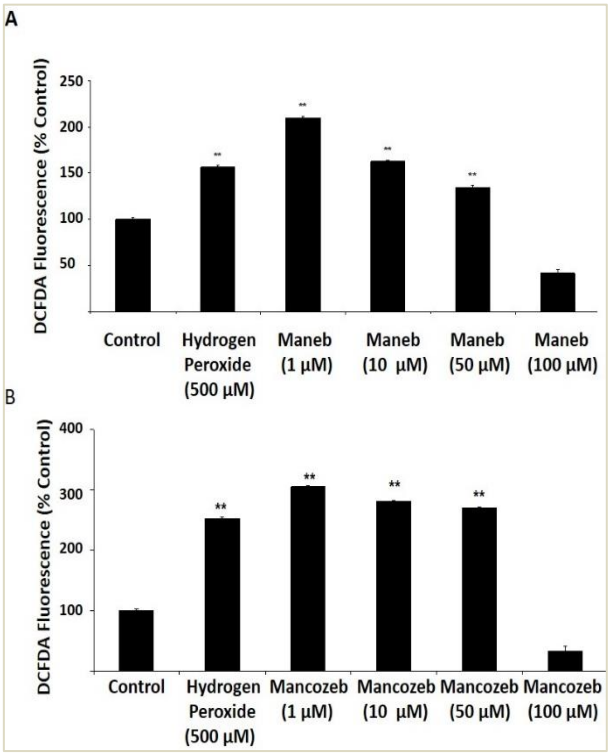

FIGURE 8. DTC-induced ROS production in SH-SY5Y cells. (A) Hydrogen peroxide (500 μM) induced a time-dependent increase in ROS production as determined by DCF-DA assay. A dose-dependent increase in ROS production was noted with (A) maneb and (B) mancozeb. Data are expressed as mean ± SD (n = 3). *, $p < 0.05$; **, $p < 0.01$, compared with control.

than zinc-containing zineb [6]. The true extent of the involvement of either component cannot be determined since it is unclear if the metal ions are detached from the organic backbone to cause toxicity or they remain attached. Manganese itself is a neurotoxin and causes oxidative stress and cell death in glial and neuronal cell lines [35], and clinically can lead to an extrapyramidal syndrome that shows some parkinsonian features [36, 37]. High level manganese exposure may lead to manganism with features similar to PD, but manganese typically damages the globus pallidus and striatum rather than the substantia nigra as in PD [37-39]. Although the molecular and cellular mechanisms of manganese toxicity are not clear, it is suggested that manganese exerts cellular toxicity through ROS generation (either direct or indirect) [40], disrupts iron and Ca^{2+} homeostasis [41, 42], causes direct oxidation of biological molecules like dopamine [43], and accumulates in mitochondria and generates ROS through disruption of oxidative phosphorylation [44]. At the doses used in the current study and given the relatively acute nature of the exposure, it is unclear if maneb or mancozeb would be able to cause neuronal cell death in vivo, other than at very high doses.

Changes in mitochondrial function are critical for cell survival as deficiency of the mitochondrial respiratory chain may cause decreased ATP synthesis, ROS generation leading to oxidative stress and mitochondrial depolarization, and eventually to cell death [5]. Aging of the nervous system is often associated with mitochondrial dysfunction [45], and evidence links mitochondrial dysfunction with PD, including a quantitative loss of complex I activity in the brain in sporadic PD patients [46]. Both rotenone and MPP^+ selectively inhibit complex I and produce several features of PD, thus providing evidence that envi-

ronmental chemical exposure, oxidative stress, and a complex I deficiency might underlie PD [47]. If a chemical directly disturbs mitochondrial function, it can exert its action by disrupting mitochondrial maintenance, localization, and active transport, which is required in neurons to deliver mitochondria to the sites of increased energy requirement [48]. Our data suggest that maneb and mancozeb do not affect complex I, II, or IV activities, but rather specifically disrupt complex III activity (**Table 3**). The measured reaction in the complex III assay is the spontaneous oxidation of substrate ubiquinol-2 (UQ-2) with cytochrome c (cyt c) as the electron acceptor, the assay measuring the increase in absorbance at 550 nm due to cyt c reduction. When maneb is added to this reaction the rate of reduction of cyt c (III) to cyt c (II) is decreased suggesting that maneb is able to block the transfer of electrons between UQ-2 and cyt c (III), possibly either by having a higher affinity for the electron than cyt c (III) and so acting as the acceptor, or by preventing the oxidation of UQ-2 or the reduction of cyt c (III) to cyt c (II). This inhibition of mitochondrial complex III may lead to the elevation of ROS seen on exposure to maneb and mancozeb. Depolarization of mitochondria interferes with electron transport and respiration [49], and as such, it can be assumed that these chemicals do not directly lead to changes in intrinsic components of mitochondrial bioenergetics such as mitochondrial membrane potential which in turn affects mitochondrial transport and distribution. Despite this effect on mitochondria, a key integrator in the pathogenesis of PD, there does not appear to be an involvement of α-synuclein suggesting that DTCs do not contribute directly to typical PD features [50].

Previous studies have suggested that melanized neurons in PD brain show evidence of autophagic degeneration [51]. In this study, the induction of autophagy was evaluated; however, it is unclear whether the accumulation of autophagic/lysosomal vacuoles in response to chemical treatment represents up-regulation or blockage of autophagy as 3-MA did not affect toxicity. The upregulation of LAMP1/2 and lysosomal enlargement would suggest that there is altered lysosomal activity in response to chemical treatment, possibly as a response to the formation of oxidized proteins, in the form of chaperone-mediated autophagy (CMA). Since neurodegeneration can be caused by neural tissue-specific knockout of autophagy genes, it is possible that in the current context, autophagy may be an attempt to remove damaged proteins, though the extensive cell death seen following chemical treatment may indicate that this is not effective when the chemical dose is high.

LAMP-1 and LAMP-2 are highly glycosylated lysosomal membrane proteins which play an important role in CMA [52]. LAMP1/2 down-regulation has been linked with increased sensitivity to lysosomal cell death [15], and results from the current study showed a significant increase in LAMP1 and LAMP2 levels in response to maneb and mancozeb treatment. An increase in the levels of LAMP-2A and CMA has been observed during oxidative stress [53]. LAMP2 can substitute some of the normal functions of LAMP1, although in this study LAMP1 was similarly elevated. Absence of LAMP1 has been linked with an altered distribution of lysosomes, accumulation of autophagic structures and LC3-positive autophagic compartments, and its depletion prevents the co-localization of lysosomal and autophagosomal markers [54]. The current study would indicate that CMA may not be directly involved with maneb and mancozeb toxicity, since 3-MA fails to rescue cells following exposure and LC3-b induction is not a feature. One possibility is that subsequent to complex III inhibition, depletion of ATP leads to lysosomal abnormalities due to energy depletion. Neuronal culture systems have been used in similar studies to investigate autophagy [55, 56] with vacuole formation in axons and cell bodies. Similar results have been reported with MPP^+ treatment which increases size and number of lysosomal vacuoles [57]. The current results for maneb and mancozeb would indicate that treatment leads to energy depletion and direct damage to cell components with induction of lysosomal changes.

The mode of cell death induced by maneb and mancozeb may involve programmed necrosis involving RIP1 rather than apoptosis since caspase inhibition is without effect. Necrosis has been suggested to occur in neurodegenerative disorders such as PD and Alzheimer's disease [58], but the involvement of RIP1 remains undetermined [59]. RIP1 undergoes cleavage by caspase-8 forming two fragments, one smaller fragment and a larger fragment containing the entire kinase domain. Inhibition of the TNF-induced and NF-κB pathways is a result of RIP1 cleavage that also increases TNF-R1-associated death domain (TRADD) and FADD interactions, en-

hancing cell-death [60]. Therefore, any imbalance in caspase-8 and RIP1 may regulate the levels of uncleaved RIP1 [60]. The current results with maneb and mancozeb indicate that cleavage of RIP1 is decreased with increased levels of the full length RIP1 molecule. While a cellular necrosis pathway may be initiated by maneb and mancozeb causing complex III inhibition and mitochondrial damage, alternative pathways of cell death may also occur including DNA damage. Induction of PARP-1, a marker of cell stress and DNA damage, was seen as a late event in treated cells. Results showed a dose-dependent increase in cleaved PARP-1 (89 kDa) fragment with mancozeb and maneb for 24 h, at concentrations of 10–100 μM. PARP-1 fragment was highly expressed after 24 h, a time-point where toxicity was maximal. The absence of any effect of caspase inhibitors on this process may suggest that caspase-independent induction of PARP-1 is a late event. Similarly, the presence of up-regulation of p53 may be a late event. The p53 expression showed a dose-dependent increase in active p53 levels with mancozeb and maneb at concentrations between 10 μM and 100 μM and was more obvious at 100 μM, and p53 increased in a time-dependent manner. It has been reported that p53 may promote cell death by regulating the expression of enzymes involved in controlling the redox state of cells [61]. Consequently, if maneb and mancozeb act by initial inhibition of complex III, then an altered redox state within cells and elevation of ROS may lead to downstream activation of p53. Although several PD features in animal and cell culture models have been reproduced by using PD-linked toxins including rotenone, paraquat, and MPTP, their molecular mechanisms of action are very well known. Paraquat does not act through dopamine transporter (DAT) or inhibit complex I [62] and activate caspase-3, whereas rotenone and MPP^+, both being powerful inhibitors of complex I activity, do not activate caspase-3 [63]. Rotenone appears to induce cell death through a caspase-independent pathway in undifferentiated cells but through caspase-dependent cell death in differentiated cells [64]. Paraquat can cause oxidative stress in dopaminergic neurons of mice [65] through mitochondria-linked apoptosis, p53 induction [66], and by causing an increase in p53 levels [67]. The level of protein expression and, therefore, the mode of cell death appear to be dependent on the nature of the neurotoxic insult.

5. CONCLUSION

Maneb and mancozeb, two widely used pesticides linked to PD, appear to have their effect through inhibition of complex III of the mitochondrial respiratory chain, which may be mediated in part by the manganese moiety since zineb and nabam have reduced capacity for induction of cell death. This mitochondrial inhibition leads to ROS production and mitochondrial damage with lysosomal changes and cell death potentially through programmed necrosis. Although capable of producing some features of the cell death observed in PD, mancozeb and maneb failed to induce changes in α-synuclein, suggesting that typical PD may not be associated with exposure to these chemicals.

ACKNOWLEDGMENTS

We thank Dr. Alex Laude at the Newcastle University Bio-Imaging facility for help with confocal microscopy. This work was supported by the UK Health Protection Agency/Public Health England, the Department of Health Policy Research Program, and the National Institutes of Health Research. R.W.T. is funded by a Wellcome Trust Strategic Award (096919/Z/11/Z). Antibodies to LAMP1 and LAMP2 created by JT August and JEK. Hildreth were obtained from the Developmental Studies Hybridoma Bank which is developed under the auspices of the NICHD and maintained by the University of Iowa, Department of Biology, Iowa City, IA 52242, USA. The research was funded by the National Institute for Health Research Health Protection Research Unit (NIHR HPRU) in Chemical and Radiation Threats and Hazards in partnership with Public Health England (PHE). The views expressed are those of the author(s) and not necessarily those of the NHS, the NIHR, the Department of Health, or Public Health England. The authors declare no conflicts of interest.

REFERENCES

1. Zhou Y, Shie FS, Piccardo P, Montine TJ, Zhang J. Proteasomal inhibition induced by manganese ethylene-bis-dithiocarbamate: relevance to Parkinson's disease. *Neuroscience*

2004; 128(2):281–91.
2. Meco G, Bonifati V, Vanacore N, Fabrizio E. Parkinsonism after chronic exposure to the fungicide maneb (manganese ethylene-bis-dithiocarbamate). *Scand J Work Environ Health* 1994; 20(4):301–5.
3. Wang A, Costello S, Cockburn M, Zhang X, Bronstein J, Ritz B. Parkinson's disease risk from ambient exposure to pesticides. *Eur J Epidemiol* 2011; 26(7):547–55. doi: 10.1007/s10654-011-9574-5.
4. Barlow BK, Lee DW, Cory-Slechta DA, Opanashuk LA. Modulation of antioxidant defense systems by the environmental pesticide maneb in dopaminergic cells. *Neurotoxicology* 2005; 26(1):63–75.
5. Drechsel DA, Patel M. Role of reactive oxygen species in the neurotoxicity of environmental agents implicated in Parkinson's disease. *Free Radic Biol Med* 2008; 44(11):1873–86.
6. Vaccari A, Saba P, Mocci I, Ruiu S. Dithiocarbamate pesticides affect glutamate transport in brain synaptic vesicles. *J Pharmacol Exp Ther* 1999; 288(1):1–5.
7. Langston JW, Ballard P, Tetrud JW, Irwin I. Chronic parkinsonism in humans due to a product of meperidine-analog synthesis. *Science* 1983; 219(4587):979–80.
8. Davis GC, Williams AC, Markey SP, Ebert MH, Caine ED, Reichert CM, et al. Chronic parkinsonism secondary to intravenous injection of meperidine analogues. *Psychiatry Res* 1979; 1(3):249–54.
9. Zhang J, Fitsanakis VA, Gu G, Jing D, Ao M, Amarnath V, et al. Manganese ethylene-bis-dithiocarbamate and selective dopaminergic neurodegeneration in rat: a link through mitochondrial dysfunction. *J Neurochem* 2003; 84(2):336–46.
10. Domico LM, Zeevalk GD, Bernard LP, Cooper KR. Acute neurotoxic effects of mancozeb and maneb in mesencephalic neuronal cultures are associated with mitochondrial dysfunction. *Neurotoxicology* 2006; 27(5):816–25. doi: 10.1016/j.neuro.2006.07.009.
11. Kametaka S, Matsuura A, Wada Y, Ohsumi Y. Structural and functional analyses of APG5, a gene involved in autophagy in yeast. *Gene* 1996; 178(1–2):139–43.
12. Kuma A, Hatano M, Matsui M, Yamamoto A, Nakaya H, Yoshimori T, et al. The role of autophagy during the early neonatal starvation period. *Nature* 2004; 432(7020):1032–6.
13. Pyo JO, Jang MH, Kwon YK, Lee HJ, Jun JI, Woo HN, et al. Essential roles of Atg5 and FADD in autophagic cell death: dissection of autophagic cell death into vacuole formation and cell death. *J Biol Chem* 2005; 280(21):20722–9. doi: 10.1074/jbc.M413934200.
14. Gonzalez-Polo RA, Boya P, Pauleau AL, Jalil A, Larochette N, Souquere S, et al. The apoptosis/autophagy paradox: autophagic vacuolization before apoptotic death. *J Cell Sci* 2005; 118(Pt 14):3091–102.
15. Fehrenbacher N, Bastholm L, Kirkegaard-Sorensen T, Rafn B, Bottzauw T, Nielsen C, et al. Sensitization to the lysosomal cell death pathway by oncogene-induced down-regulation of lysosome-associated membrane proteins 1 and 2. *Cancer Res* 2008; 68(16):6623–33.
16. Bilski P, Belanger AG, Chignell CF. Photosensitized oxidation of 2',7'-dichlorofluorescin: singlet oxygen does not contribute to the formation of fluorescent oxidation product 2',7'-dichlorofluorescein. *Free Radic Biol Med* 2002; 33(7):938–46.
17. Myhre O, Andersen JM, Aarnes H, Fonnum F. Evaluation of the probes 2',7'-dichlorofluorescin diacetate, luminol, and lucigenin as indicators of reactive species formation. *Biochem Pharmacol* 2003; 65(10):1575–82.
18. Krohn AJ, Wahlbrink T, Prehn JH. Mitochondrial depolarization is not required for neuronal apoptosis. *J Neurosci* 1999; 19(17):7394–404.
19. Gunter TE, Pfeiffer DR. Mechanisms by which mitochondria transport calcium. *Amer J Physiol* 1990; 258(5 Pt 1):C755–86.
20. Kirby DM, Thorburn DR, Turnbull DM, Taylor RW. Biochemical assays of respiratory chain complex activity. *Methods Cell Biol* 2007; 80:93–119. doi: 10.1016/S0091-679X(06)80004-X.
21. Birch-Machin MA, Briggs HL, Saborido AA, Bindoff LA, Turnbull DM. An evaluation of the measurement of the activities of complexes I–IV in the respiratory chain of human skeletal muscle mitochondria. *Biochem Med Metab Biol* 1994; 51(1):35–42.
22. Amstad PA, Yu G, Johnson GL, Lee BW,

Dhawan S, Phelps DJ. Detection of caspase activation in situ by fluorochrome-labeled caspase inhibitors. *Biotechniques* 2001; 31(3):608–10, 12, 14, passim.
23. McCarthy NJ, Whyte MK, Gilbert CS, Evan GI. Inhibition of Ced-3/ICE-related proteases does not prevent cell death induced by oncogenes, DNA damage, or the Bcl-2 homologue Bak. *J Cell Biol* 1997; 136(1):215–27.
24. Villa PG, Henzel WJ, Sensenbrenner M, Henderson CE, Pettmann B. Calpain inhibitors, but not caspase inhibitors, prevent actin proteolysis and DNA fragmentation during apoptosis. *J Cell Sci* 1998; 111 (Pt 6):713–22.
25. Shimizu S, Kanaseki T, Mizushima N, Mizuta T, Arakawa-Kobayashi S, Thompson CB, et al. Role of Bcl-2 family proteins in a non-apoptotic programmed cell death dependent on autophagy genes. *Nat Cell Biol* 2004; 6(12):1221–8.
26. Hosokawa N, Hara Y, Mizushima N. Generation of cell lines with tetracycline-regulated autophagy and a role for autophagy in controlling cell size. *FEBS Lett* 2006; 580(11):2623–9. doi: 10.1016/j.febslet.2006.04.008.
27. Degterev A, Hitomi J, Germscheid M, Ch'en IL, Korkina O, Teng X, et al. Identification of RIP1 kinase as a specific cellular target of necrostatins. *Nature Chem Biol* 2008; 4(5):313–21.
28. Gomes A, Fernandes E, Lima JL. Fluorescence probes used for detection of reactive oxygen species. *J Biochem Biophys Methods* 2005; 65(2–3):45–80.
29. Satoh MS, Lindahl T. Role of poly(ADP-ribose) formation in DNA repair. *Nature* 1992; 356(6367):356–8.
30. Lazebnik YA, Kaufmann SH, Desnoyers S, Poirier GG, Earnshaw WC. Cleavage of poly(ADP-ribose) polymerase by a proteinase with properties like ICE. *Nature* 1994; 371(6495):346–7.
31. Nicholson DW, Ali A, Thornberry NA, Vaillancourt JP, Ding CK, Gallant M, et al. Identification and inhibition of the ICE/CED-3 protease necessary for mammalian apoptosis. *Nature* 1995; 376(6535):37–43. doi: 10.1038/376037a0.
32. Morrison RS, Kinoshita Y. The role of p53 in neuronal cell death. *Cell Death Diff* 2000; 7(10):868–79. doi: 10.1038/sj.cdd.4400741.
33. Watabe M, Nakaki T. Rotenone induces apoptosis via activation of bad in human dopaminergic SH-SY5Y cells. *J Pharmacol Exp Ther* 2004; 311(3):948–53.
34. Borland MK, Trimmer PA, Rubinstein JD, Keeney PM, Mohanakumar K, Liu L, et al. Chronic, low-dose rotenone reproduces Lewy neurites found in early stages of Parkinson's disease, reduces mitochondrial movement and slowly kills differentiated SH-SY5Y neural cells. *Mol Neurodegener* 2008; 3:21.
35. Dukhande VV, Malthankar-Phatak GH, Hugus JJ, Daniels CK, Lai JC. Manganese-induced neurotoxicity is differentially enhanced by glutathione depletion in astrocytoma and neuroblastoma cells. *Neurochem Res* 2006; 31(11):1349–57.
36. Calne DB, Chu NS, Huang CC, Lu CS, Olanow W. Manganism and idiopathic parkinsonism: similarities and differences. *Neurology* 1994; 44(9):1583–6.
37. Racette BA, Searles Nielsen S, Criswell SR, Sheppard L, Seixas N, Warden MN, et al. Dose-dependent progression of parkinsonism in manganese-exposed welders. *Neurology* 2017; 88(4):344–51. doi: 10.1212/WNL.0000000000003533.
38. Dobson AW, Erikson KM, Aschner M. Manganese neurotoxicity. *Ann N Y Acad Sci* 2004; 1012:115–28.
39. Levy BS, Nassetta WJ. Neurologic effects of manganese in humans: a review. *Int J Occup Environ Health* 2003; 9(2):153–63.
40. Sidoryk-Wegrzynowicz M, Aschner M. Manganese toxicity in the central nervous system: the glutamine/glutamate-gamma-aminobutyric acid cycle. *J Intern Med* 2013; 273(5):466–77. doi: 10.1111/joim.12040.
41. Gavin CE, Gunter KK, Gunter TE. Manganese and calcium efflux kinetics in brain mitochondria: relevance to manganese toxicity. *Biochem J* 1990; 266(2):329–34.
42. Zheng W, Zhao Q. Iron overload following manganese exposure in cultured neuronal, but not neuroglial cells. *Brain Res* 2001; 897(1–2):175–9.
43. Archibald FS, Tyree C. Manganese poisoning and the attack of trivalent manganese upon catecholamines. *Arch Biochem Biophys* 1987; 256(2):638–50.

44. Gunter TE, Gavin CE, Aschner M, Gunter KK. Speciation of manganese in cells and mitochondria: a search for the proximal cause of manganese neurotoxicity. *Neurotoxicology* 2006; 27(5):765–76.
45. Melov S. Modeling mitochondrial function in aging neurons. *Trends Neurosci* 2004; 27(10):601–6.
46. Schapira AH, Cooper JM, Dexter D, Jenner P, Clark JB, Marsden CD. Mitochondrial complex I deficiency in Parkinson's disease. *Lancet* 1989; 1(8649):1269.
47. Schmidt WJ, Alam M. Controversies on new animal models of Parkinson's disease pro and con: the rotenone model of Parkinson's disease (PD). *J Neural Transm Suppl* 2006; (70):273–6.
48. Van Laar VS, Berman SB. Mitochondrial dynamics in Parkinson's disease. *Exp Neurol* 2009; 218(2):247–56.
49. Mookherjee P, Quintanilla R, Roh MS, Zmijewska AA, Jope RS, Johnson GV. Mitochondrial-targeted active Akt protects SH-SY5Y neuroblastoma cells from staurosporine-induced apoptotic cell death. *J Cell Biochem* 2007; 102(1):196–210.
50. Di Monte D, Irwin I, Kupsch A, Cooper S, DeLanney LE, Langston JW. Diethyldithiocarbamate and disulfiram inhibit MPP^+ and dopamine uptake by striatal synaptosomes. *Eur J Pharmacol* 1989; 166(1):23–9.
51. Anglade P, Vyas S, Javoy-Agid F, Herrero MT, Michel PP, Marquez J, et al. Apoptosis and autophagy in nigral neurons of patients with Parkinson's disease. *Histol Histopathol* 1997; 12(1):25–31.
52. Kiffin R, Kaushik S, Zeng M, Bandyopadhyay U, Zhang C, Massey AC, et al. Altered dynamics of the lysosomal receptor for chaperone-mediated autophagy with age. *J Cell Sci* 2007; 120(Pt 5):782–91.
53. Kiffin R, Christian C, Knecht E, Cuervo AM. Activation of chaperone-mediated autophagy during oxidative stress. *Mol Biol Cell* 2004; 15(11):4829–40.
54. Eskelinen EL, Saftig P. Autophagy: a lysosomal degradation pathway with a central role in health and disease. *Biochim Biophys Acta* 2009; 1793(4):664–73. doi: 10.1016/j.bbamcr.2008.07.014.
55. Hollenbeck PJ. Products of endocytosis and autophagy are retrieved from axons by regulated retrograde organelle transport. *J Cell Biol* 1993; 121(2):305–15.
56. Cubells JF, Rayport S, Rajendran G, Sulzer D. Methamphetamine neurotoxicity involves vacuolation of endocytic organelles and dopamine-dependent intracellular oxidative stress. *J Neurosci* 1994; 14(4):2260–71.
57. Zhu Y, Hoell P, Ahlemeyer B, Sure U, Bertalanffy H, Krieglstein J. Implication of PTEN in production of reactive oxygen species and neuronal death in in vitro models of stroke and Parkinson's disease. *Neurochem Int* 2007; 50(3):507–16.
58. Kitanaka A, Suzuki T, Ito C, Nishigaki H, Coustan-Smith E, Tanaka T, et al. CD38-mediated signaling events in murine pro-B cells expressing human CD38 with or without its cytoplasmic domain. *J Immunol* 1999; 162(4):1952–8.
59. Kelliher MA, Grimm S, Ishida Y, Kuo F, Stanger BZ, Leder P. The death domain kinase RIP mediates the TNF-induced NF-kappaB signal. *Immunity* 1998; 8(3):297–303.
60. Christofferson DE, Li Y, Yuan J. Control of life-or-death decisions by RIP1 kinase. *Ann Rev Physiol* 2014; 76:129–50. doi: 10.1146/annurev-physiol-021113-170259.
61. Polyak K, Xia Y, Zweier JL, Kinzler KW, Vogelstein B. A model for p53-induced apoptosis. *Nature* 1997; 389(6648):300–5.
62. Richardson JR, Quan Y, Sherer TB, Greenamyre JT, Miller GW. Paraquat neurotoxicity is distinct from that of MPTP and rotenone. *Toxicol Sci* 2005; 88(1):193–201. doi: 10.1093/toxsci/kfi304.
63. Ramachandiran S, Hansen JM, Jones DP, Richardson JR, Miller GW. Divergent mechanisms of paraquat, MPP^+, and rotenone toxicity: oxidation of thioredoxin and caspase-3 activation. *Toxicol Sci* 2007; 95(1):163–71.
64. Li J, Spletter ML, Johnson DA, Wright LS, Svendsen CN, Johnson JA. Rotenone-induced caspase 9/3-independent and -dependent cell death in undifferentiated and differentiated human neural stem cells. *J Neurochem* 2005; 92(3):462–76.
65. McCormack AL, Atienza JG, Johnston LC, Andersen JK, Vu S, Di Monte DA. Role of

oxidative stress in paraquat-induced dopaminergic cell degeneration. *J Neurochem* 2005; 93(4):1030–7.
66. Ueda S, Masutani H, Nakamura H, Tanaka T, Ueno M, Yodoi J. Redox control of cell death. *Antioxid Redox Signal* 2002; 4(3):405–14.
67. Takeyama N, Tanaka T, Yabuki T, Nakatani T. The involvement of p53 in paraquat-induced apoptosis in human lung epithelial-like cells. *Int J Toxicol* 2004; 23(1):33–40.